

Active-site MMP-selective antibody inhibitors discovered from convex paratope synthetic libraries

Dong Hyun Nam^a, Carlos Rodriguez^a, Albert G. Remacle^b, Alex Y. Strongin^b, and Xin Ge^{a,1}

^aDepartment of Chemical and Environmental Engineering, University of California, Riverside, CA 92521; and ^bInflammatory and Infectious Disease Center and Cancer Research Center, Sanford Burnham Prebys Medical Discovery Institute, La Jolla, CA 92037

Edited by K. Dane Wittrup, Adimab, LLC, Lebanon, NH, and accepted by Editorial Board Member David Baker November 21, 2016 (received for review June 9, 2016)

Proteases are frequent pharmacological targets, and their inhibitors are valuable drugs in multiple pathologies. The catalytic mechanism and the active-site fold, however, are largely conserved among the protease classes, making the development of the selective inhibitors exceedingly challenging. In our departure from the conventional strategies, we reviewed the structure of known camelid inhibitory antibodies, which block enzyme activities via their unusually long, convex-shaped paratopes. We synthesized the human Fab antibody library (over 1.25×10^9 individual variants) that carried the extended, 23- to 27-residue, complementarity-determining region (CDR)-H3 segments. As a proof of principle, we used the catalytic domain of matrix metalloproteinase-14 (MMP-14), a promalignant protease and a drug target in cancer, as bait. In our screens, we identified 20 binders, of which 14 performed as potent and selective inhibitors of MMP-14 rather than as broad-specificity antagonists. Specifically, Fab 3A2 bound to MMP-14 in the vicinity of the active pocket with a high 4.8 nM affinity and was similarly efficient (9.7 nM) in inhibiting the protease cleavage activity. We suggest that the convex paratope antibody libraries described here could be readily generalized to facilitate the design of the antibody inhibitors to many additional enzymes.

inhibitory antibody | long CDR | synthetic library | convex paratope | MMP

As key cellular proteinases, matrix metalloproteinase (MMP) family members control various physiological and pathological processes. Multiple diseases are associated with altered MMP expression and aberrant proteolysis, including cancer (1), wound healing (2), inflammatory diseases (3, 4), neurological pain (5, 6), and hypertension (7). There is consensus among researchers that the individual MMPs are promising drug targets in diversified pathologies and that inhibitor specificity is required for selective and successful MMP therapies (8–10).

However, achieving target specificity and selectivity in small-molecule MMP inhibitors is remarkably challenging (11, 12). Because the catalytic mechanism and catalytic domain fold are conserved among the MMP/ADAM (a disintegrin and metalloproteinase)/ADAMTS (ADAM with thrombospondin motifs) superfamily members, the available small-molecule inhibitors (most frequently, active-site zinc-chelating hydroxamates) target multiple proteinases, resulting in off-target side effects (8, 12–14). This aspect is problematic, given that some MMPs (e.g., MMP-14) are always protumorigenic, whereas some other MMPs are antitumorigenic in certain cancer microenvironments (15, 16). As a result, broad-spectrum hydroxamates failed in cancer clinical trials due to their low overall efficacy and side effects (13). Alternatively, antibody-based MMP inhibitors are emerging as both research tools and potential therapeutic agents (10, 17–21) because of (i) high affinity and specificity due to the large antigen–antibody interaction area and multiple complementarity-determining regions (CDRs), (ii) long half-life and well-defined action mechanisms, (iii) low immunogenicity and toxicity, and (iv) multiple MMPs potentially targetable by antibodies (9).

Natural protease inhibitors exhibit a convex-shaped conformation that inserts into the enzyme active site and blocks the substrate access and/or catalytic function (22). However, there is a low probability of generating antibodies with the convex antigen-binding sites

(paratopes) from naive or immunized human or murine antibody libraries. The proteolytic pocket is often buried inside a major cleft or concave enzyme structure, and, as such, it is normally inaccessible by the cave-like, grooved, or flat antigen-binding surface in human and murine antibodies (23). In contrast, dromedary antibodies are enriched in the long CDR-H3s encoding the extended convex-shaped paratopes and, intriguingly, a large proportion of antibodies isolated from camels and llamas, compared with human and murine antibodies, bind the active-site pockets and inhibit enzymatic reactions (24–26). However, the camelid antibodies would evoke an immune response in humans, and the availability of these animals is limited.

With the hypothesis that convex paratopes are inhibitory, we designed human Fab libraries in which the long, convex-shaped, camelid-like paratopes were incorporated into the human antibody scaffold (27) (Fig. S1). In our current proof-of-principle study, we screened these libraries for the inhibitors of MMP-14, a proinvasive and prometastatic human proteinase (28, 29). As a result of our screens, we isolated a panel of selective Fabs with a high inhibitory potency against MMP-14. We are now confident that these libraries and similar libraries that exhibit the long, convex paratopes will be a valuable source of the inhibitory antibodies capable of targeting multiple additional enzymes, the active pockets of which are not readily accessible by the conventional human antibodies.

Results

Design and Construction of Long CDR-H3 Synthetic Fab Libraries. A large proportion of camelid heavy-chain antibodies ($V_{\text{H}}\text{Hs}$) exhibit enzyme-inhibiting functions (24, 25). Structure studies suggest that

Significance

The matrix metalloproteinase (MMP) family members are promising drug targets in diversified pathologies. Clinical trial failures taught us that selective, rather than broad-specificity, inhibitors are required for successful MMP therapies. Achieving target selectivity with small-molecule MMP inhibitors, however, is exceedingly difficult. Because the antigen-binding sites in conventional antibodies are predominantly incompatible with the concave reaction pockets of MMPs, design of inhibitory antibodies, an attractive alternative for selective inhibition, is also challenging. We synthesized human antibody libraries encoding extended convex antigen-binding sites and isolated a panel of inhibitory Fabs that selectively and efficiently inhibited MMP-14, a promising drug target in cancer. The pipeline we established can now be readily applied for the generation of inhibitory antibodies targeting multiple additional enzymes besides MMPs alone.

Author contributions: D.H.N. and X.G. designed research; D.H.N., C.R., and A.G.R. performed research; D.H.N., A.G.R., A.Y.S., and X.G. analyzed data; and D.H.N., A.G.R., A.Y.S., and X.G. wrote the paper.

The authors declare no conflict of interest.

This article is a PNAS Direct Submission. K.D.W. is a Guest Editor invited by the Editorial Board.

¹To whom correspondence should be addressed. Email: xge@engr.ucr.edu.

This article contains supporting information online at www.pnas.org/lookup/suppl/doi:10.1073/pnas.1609375114/-DCSupplemental.

The 20 selected Fabs were produced in *Escherichia coli* periplasmic space with a typical yield of the purified proteins of 0.5–2 mg/L medium (Fig. S5A). Size exclusion chromatography confirmed that the isolated Fab samples were highly soluble and present as monomers in solution, without detectable aggregation (Fig. S5B). After storage at 4 °C for 1 mo, purified Fab samples were still stable without visible aggregates or degradation as determined by SDS/PAGE (Fig. S5C).

The binding affinity of the purified Fabs with MMP-14 was measured using ELISA. The binding EC_{50} value of the samples was in a 3.8 to 1,600 nM range (Table 1). The most efficient binders included 3A2 (3.8 nM), 3D9 (6.4 nM), and 32E10 (9.7 nM), and the EC_{50} values of the additional five Fabs were between 24 and 51 nM (Fig. 1A, Table 1, and Fig. S6). Fourteen (70%) of the 20 Fabs we purified inhibited MMP-14 proteolysis of the fluorescent peptide substrate (7-methoxycoumarin-4-yl)Acetyl-Lys-Pro-Leu-Gly-Leu-(3-[2,4-dinitrophenyl]-L-2,3-diaminopropionyl)-Ala-Arg-NH₂, with IC_{50} values between 9.7 nM and 8 μ M (Table 1). The presence of 70% of the inhibitory clones among the binders is remarkably high, especially if compared with previous studies of the inhibitory antibodies (hit rates of 2.5% and 17%) (17, 36). The inhibition IC_{50} values of Fabs 3A2, 3E2, and 3D9 were 9.7 nM, 42 nM, and 61 nM, respectively, and the IC_{50} values of three additional Fabs were in 240–420 nM range (Fig. 1A and Table 1). Fab 3E9, the most enriched clone we isolated through phage panning (22 repeated sequences), showed a moderate, 51 nM binding capacity, but its inhibitory potency was low (IC_{50} = 6.0 μ M) (Table 1 and Fig. S6A). The enrichment of this clone was likely a result of a high growth rate and/or high expression level relative to other Fab clones. Similarly, a few high-affinity Fabs [e.g., 32E10 (EC_{50} = 9.7 nM)] did not inhibit MMP-14, suggesting that efficient binding

does not directly correlate with high inhibitory potency of the antibody (Fig. S6B). To test whether the most promising inhibitory Fabs are resistant to MMP-14 proteolysis (37), Fabs 3A2, 3E2, 3D9, and 2B5 were incubated with MMP-14 (at an enzyme/antibody molar ratio of 1:5 or 1:10) at pH 7.5 and 37 °C for 1 or 16 h. No significant degradation of the antibodies was observed under these conditions (Fig. S7).

In a control experiment, in the course of phage panning, we used a highly diversified antibody library (3×10^{10} variants) exhibiting the normal 1- to 17-residue CDR-H3s (35) and phage elution steps with n-TIMP-2. This experiment resulted in six individual Fabs bound to MMP-14 with a low nanomolar affinity; however, none was inhibitory even at 2–4 μ M (Table 1). These findings strongly support the expectation that the convex-shaped paratopes formed by the long CDR-H3 segments play an essential role in generating the inhibitory antibodies.

Because selectivity is the prime parameter for the MMP inhibitors, we next assessed if the most promising Fabs would cross-react with other MMPs. According to the ELISA results, all of the six Fabs we tested were highly selective for MMP-14. Indeed, Fabs 3A2, 3E2, 3D9, and 2B5 were incapable of binding to MMP-2 or MMP-9 even at a high concentration of 500 nM. The two other Fabs, 33D2 and 3G9, were ~10- to 20-fold more selective for MMP-14 relative to MMP-2 and MMP-9 (Fig. 1B).

Fab 3A2 Is a Highly Potent Competitive Selective Inhibitor of MMP-14.

The most efficient inhibitor, Fab 3A2, was studied in a more detail to determine both its inhibitory mechanism and its binding mode. The binding kinetics of Fab 3A2 to MMP-14 were examined using surface plasmon resonance spectroscopy (Fig. 2A). A concentration-dependent saturable binding of 10–20 nM Fab 3A2 to immobilized MMP-14 was observed. Apparent equilibrium binding constants were determined with an average kinetic association coefficient (k_{on}) equal to $3.68 \times 10^5 \text{ M}^{-1} \cdot \text{s}^{-1}$ and an average kinetic dissociation coefficient (k_{off}) of $1.79 \times 10^{-3} \text{ s}^{-1}$. The equilibrium dissociation constant (K_d) calculated from the k_{off}/k_{on} ratio was 4.85 nM, and this value agreed well with the ELISA data (Fig. 1A).

The IC_{50} value of Fab 3A2 was 9.7 ± 1.2 nM and similar to the IC_{50} value of n-TIMP-2 (IC_{50} = 5.1 ± 2.4 nM) and GM6001, a potent, albeit nonselective, hydroxamate inhibitor of MMPs (IC_{50} = 2.1 ± 0.6 nM) (Fig. 2B). At 500 nM, Fab 3A2 completely inhibited MMP-14 (98%), but not MMP-2 or MMP-9 (0.2% and 2.5% inhibition, respectively) (Fig. 2C). At the similar conditions, n-TIMP-2 and GM6001 inhibited MMP-2/MMP-9/MMP-14 nonselectively (83–100% inhibition), confirming that they are broad-spectrum inhibitors of the MMP family (38, 39).

Competitive ELISA results (Fig. 2D) indicated that increasing concentrations of n-TIMP-2 reduced the binding of Fab 3A2 to MMP-14, likely suggesting an overlap of their respective binding sites in MMP-14. To determine the type of inhibition, a series of kinetic assays in the presence of 0, 250, and 500 nM Fab 3A2 was performed. The obtained Lineweaver–Burk plots demonstrated an unchanged maximum velocity (V_{max}) and an elevated Michaelis constant (K_m) when the Fab concentration increased, indicating that Fab 3A2 performed as a competitive inhibitor of MMP-14 proteolytic activity (Fig. 2E).

To identify the binding site of Fab 3A2, we performed Ala scanning mutagenesis of MMP-14. Eight residue positions (T190, F198, Y203, F204, N229, N231, S251, and F260) were selected for Ala substitution, based on the following criteria: (i) distinct in MMP-14 relative to MMP-2 and MMP-9 (Fig. S8A), (ii) within a distance of 15 Å from the catalytic Zn²⁺, (iii) exhibiting an exposed respective side chain, and (iv) near the S1' subsite (40, 41). The resulting MMP-14 mutants were expressed in the periplasmic space of *E. coli* (42). Compared with wild-type MMP-14, these MMP-14 mutants exhibited reduced, albeit still substantial, specific activity (0.4–6.6% relative to the wild type), which was used as the basis for our inhibition measurements (Fig. S8B). ELISA and

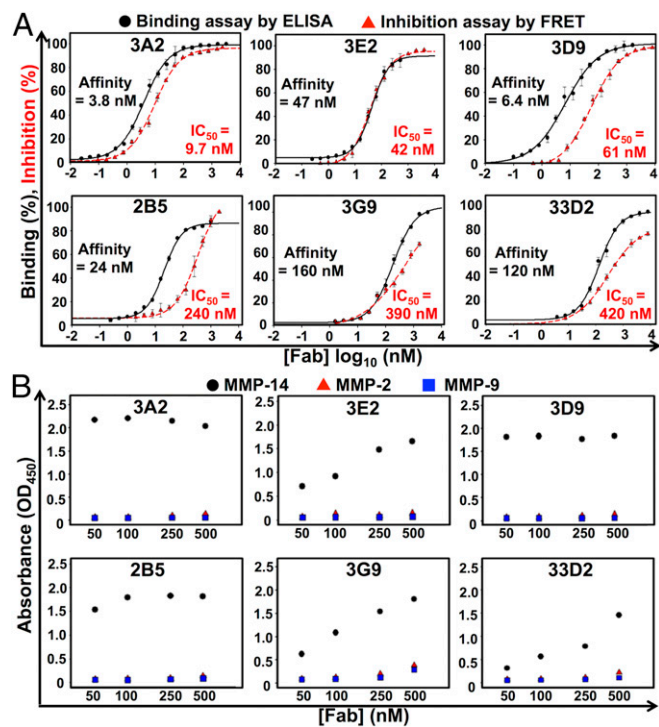


Fig. 1. Biochemical characterizations of representative high-potency inhibitory Fabs. (A) Dose–response curves of binding affinity (black) and IC_{50} (red) values of purified Fabs. Quenched-fluorescent substrate peptide (1 μ M) and 1 nM catalytic domain MMP-14 (1 nM) were used in FRET inhibition assays. Error bars represent the SD of triplicate experiments. (B) Binding selectivity toward MMP-14 (black circles) over MMP-2 (red triangles) and MMP-9 (blue squares) tested by ELISA.

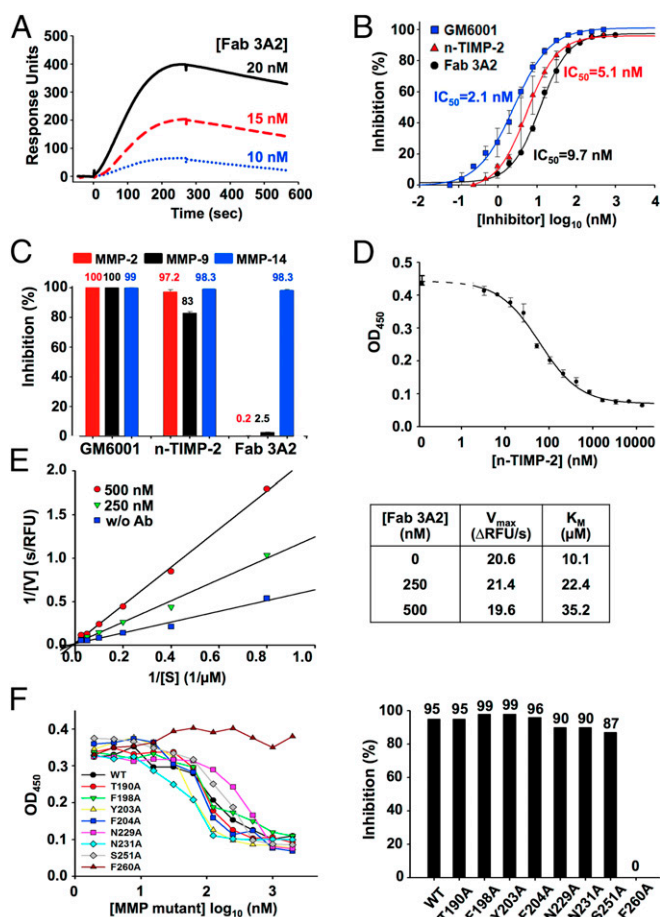


Fig. 2. Binding affinity and inhibition potency measurements, inhibitor type determination, and epitope mapping of Fab 3A2. (A) Binding kinetics of 10 nM (blue dotted line), 15 nM (red dashed line), and 20 nM (black solid line) Fab 3A2 to catalytic domain MMP-14 (cdMMP-14) measured by surface plasmon resonance. On average, $k_{on} = 3.68 \times 10^5$ ($M^{-1}s^{-1}$), $k_{off} = 1.79 \times 10^{-3}$ (s^{-1}), and $K_d = 4.85$ nM. (B) Fab 3A2 inhibited cdMMP-14 proteolytic activity on the peptide substrate with a potency of 9.7 ± 1.2 nM, the same order of magnitude as n-TIMP-2 (5.1 ± 2.4 nM) and GM6001 (2.1 ± 0.6 nM). (C) Inhibition selectivity tests of Fab 3A2, GM6001, and n-TIMP-2 toward MMP-2/MMP-9/MMP-14. In contrast to GM6001 and n-TIMP-2, Fab 3A2 showed selectivity to MMP-14 and did not inhibit MMP-2/MMP-9. (D) Competitive ELISA of Fab 3A2 with n-TIMP-2. Serially diluted n-TIMP-2 samples were incubated with 10 nM Fab 3A2 in streptavidin wells coated with biotinylated cdMMP-14. The signals were generated by anti-Fab-HRP. (E, Left) Lineweaver-Burk plots of MMP-14 with 0, 250, and 500 nM Fab 3A2. RFU, relative fluorescent units. (E, Right) Calculated V_{max} and K_m are shown. (F) Epitope determination by competitive ELISA and inhibition assays. Eight MMP-14 single-site mutants were prepared by periplasmic expression without refolding. Fab 3A2 (10 nM) was incubated with increasing amounts of MMP-14 mutant on a surface coated with wild-type MMP-14. An inhibition assay was performed using 50 nM MMP-14 mutant, 5 μ M Fab 3A2, and 1 μ M quenched fluorescent substrate.

inhibition assay results showed that the performance of all these mutants, except F260A, did not differ significantly from the performance of the original MMP-14 (Fig. S8C). In contrast, the F260A MMP-14 mutant lost its ability to bind to the Fab 3A2 and, consistently, the catalytic activity of this mutant was resistant to inhibition by Fab 3A2 (Fig. 2F). Our results, especially when combined, imply that Fab 3A2 is a competitive selective inhibitor of MMP-14, that the binding site of this antibody overlaps with the binding site of TIMP-2, and that the extended CDR-H3 loop of Fab 3A2 likely accesses the F260 residue from the S1' subsite in the MMP-14 active-site pocket.

Fab 3A2 Inhibits MMP-14 Collagenolysis and Activation of the MMP-2 Proenzyme. Activation of the MMP-2 proenzyme is the most well-known function of cell-surface MMP-14 (43). To evaluate the effect of the Fab 3A2 on MMP-2 activation, we used human fibrosarcoma HT1080 cells, which produce high levels of MMP-2 naturally. To stimulate activation of the MMP-2 proenzyme by cellular MMP-14, the cells were treated with tetradecanoyl phorbol acetate, and then coincubated with Fab 3A2 or 3E9 [a weak inhibitory Fab ($IC_{50} = 6$ μ M) as a negative control] or with GM6001 (a highly potent hydroxamate MMP inhibitor as a positive control). The status of MMP-2 was next analyzed by gelatin zymography (Fig. 3A). As expected, 10 μ M GM6001 (used at a high concentration due to its low stability in aqueous solutions of cellular assays) totally repressed MMP-2 activation. Although >40% of proMMP-2 was processed when no Fab or Fab 3E9 was applied, 200 nM Fab 3A2 inhibited 82% of MMP-14-dependent MMP-2 activation in HT1080 cells. These results were consistent with the peptide inhibition assays, confirming that Fab 3A2 inhibited MMP-14 with a high potency in HT1080 cells.

Because MMP-14 is a collagenase, we then tested if Fab 3A2 affected MMP-14 collagenolysis. For these purposes, we used human mammary epithelial 184B5 cells stably transfected with MMP-14 (44). As a control, we used the original 184B5 cells, which naturally produce a low level of MMP-14. Cells were plated on a layer of type I collagen with or without the inhibitors. Following incubation for 5 d, cells were gently detached and the collagen layer was fixed and then stained using Coomassie Blue R-250 stain to visualize the degraded, unstained areas. Fig. 3B shows that collagen was almost completely degraded (<10% of collagen remained) by 184B5-MMP14 cells. As expected, GM6001, at a high concentration of 25 μ M, blocked 96% of collagenolysis. Similarly, Fab 3A2, at a low concentration of 250 nM, repressed 93% of collagenolysis in 184B5-MMP14 cells. These data suggest that Fab 3A2 performs as a potent inhibitor of MMP-14 in cell-based assays and represses MMP-14 proteolysis of its natural, physiologically relevant substrates.

Discussion

Monoclonal antibodies (mAbs) are ubiquitous in biomedical research and medicine. A variety of methodologies have been developed for recombinant antibody discovery. The design of mAbs with selective proteinase-inhibiting functions, however, remains a significant challenge because of (i) the low antigenicity of the catalytic centers that are normally buried in the enzyme globule and (ii) the lack of reliable function-based selection methods. For example, in an attempt to isolate the antibodies capable of inhibiting serpase (a membrane-associated serine protease encoded by the fibroblast activation protein gene), 40 efficiently binding single-chain variable fragment (scFv) clones were identified from a human naive scFv phage display library of over 1×10^{10} variants, but only a single scFv construct exhibited inhibition function with a micromolar range potency (36).

The inhibitor/binder ratio was significantly improved when a specific selection procedure was added to phage panning (17). Thus, the use of TIMP-2, a natural protein inhibitor of MMP-14, as a competitive eluent of the antigen-binding clones from the MMP-14 bait led to the discovery of 12 inhibitory constructs from 70 affinity clones (17% hit rate). In addition, TIMP-2 binds to the native MMP-14 enzyme rather than to the misfolded and denatured species of the proteinase. As a result, the use of TIMP-2 allows one to disregard the antibodies that bind to the denatured MMP-14 species.

Extending these findings, our current methodology combined this epitope-specific elution with a synthetic antibody library design. Our approach resulted in the identification of 14 inhibitory antibodies from the 20 isolated MMP-14 binders [i.e., with a high (70%) hit rate]. The rationale of our antibody repertoire design was based on sequence analysis of the inhibitory camelid V_H Hs

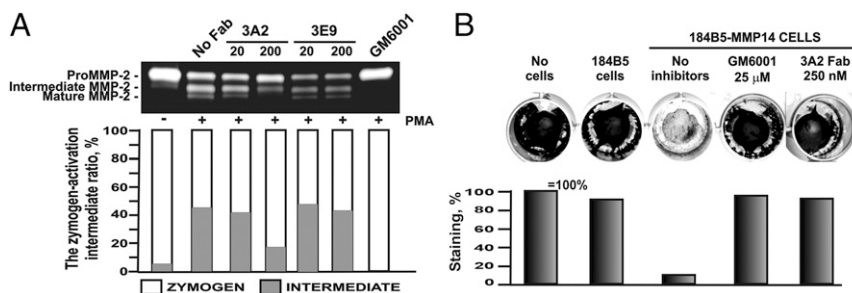


Fig. 3. Inhibition function of Fab 3A2 on MMP-14 proteolytic activities toward physiological substrates. (A) Gelatin zymography of MMP-14-dependent activation of proMMP-2. (B) Fab 3A2 inhibition on degradation of type I collagen mediated by cellular MMP-14. The intensity of the bands and collagen was quantified using the digitized images and ImageJ (NIH) software. In gelatin zymography, a proenzyme/activation intermediate ratio was expressed as the percentage of the proenzyme and the intermediate, each relative to their total amount.

and the crystal structures of the multiple $V_{\text{H}}\text{H}/\text{enzyme}$ complexes. These analyses revealed that the extended CDR-H3s provided the enlarged antigen-binding surface and convex paratopes that penetrated into the catalytic cleft and inhibited the enzymatic reaction (22, 24). In addition to the camelid single-domain antibodies, inhibitory antibodies were recently developed using antibody scaffolding of the cow. In the latter, the protruding domains encoded by the ultralong, up to 60-residue, CDR-H3s are frequent (45, 46). In agreement, structural studies of the inhibitory antibodies isolated from human naive libraries also suggested that insertion of the long CDR-H3 variable loops (up to 19 residues) into the substrate-binding pocket is required to achieve efficient inhibition of membrane type serine protease 1 (matriptase) (37, 47). Although the alternative inhibitory mechanisms are also well known, including those mechanisms that inactivate enzymes by inducing conformational changes or by blocking substrate access (48, 49), multiple inhibitory antibodies exhibit unusually long CDR-H3s, implying that the extended CDR-H3s are vital for enzyme inhibition. Therefore, in this proof-of-concept study, 23- to 27-residue-long CDR-H3s were arbitrarily designed and synthesized presumably to form convex-shaped paratopes. The presence of these long CDR-H3s is infrequent in the natural human IgGs (50). Our results clearly suggest that the constructed long CDR-H3s (but not the normal-length CDR-H3s) are inhibitory when MMP-14 was used as bait (Table 1). However, the optimal CDR-H3 length for inhibiting certain enzymes probably needs to be adjusted according to the targets (i.e., the topology of reaction pockets).

Our current study resulted in 14 inhibitory antibodies of which Fab 3A2, without any maturation, was highly potent against MMP-14. The inhibitory potency of this Fab was similar to the inhibitory potency of n-TIMP-2, the natural inhibitor of MMPs, and GM6001, one of the most effective, albeit broad-specificity, hydroxamate MMP inhibitors. However, in contrast to n-TIMP-2 or GM6001, Fab 3A2 was highly selective and did not exhibit off-target effects with other MMP family members, such as MMP-2/MMP-9. Importantly, Fab 3A2 efficiently repressed the activity of cellular MMP-14 on its physiological substrates, including MMP-2 and type I collagen. In addition to Fab 3A2, our research led to the discovery of five other potent inhibitors with promising selectivity against MMP-14, with an IC_{50} value less than 500 nM. Based on the relationship between binding affinity and inhibition potency, the 14 inhibitory Fabs isolated in this study can be grouped into four clusters (Fig. S9): group 1, the seven clones with high binding affinity and high inhibition potency, having the potential to serve as leads suitable for further characterizations; group 2, two clones with high binding affinity and low inhibition potency, presumably which paratopes partially contribute to inhibition; and groups 3 and 4, five clones with moderate or low binding affinity and moderate inhibition potency, probably binding to inhibitory epitopes with sub-optimal strengths. Overall, this inhibitory Fab panel provides a rich

pool of lead candidates for the further selection of therapeutics and fine-tuning of pharmacological properties through affinity maturation and solubility/stability improvement.

Mutagenesis of MMP-14, rather than a linear peptide approach (51), followed by the expression of mutants in the periplasm of *E. coli* (42), allowed us to map the Fab 3A2 epitope roughly in the MMP-14 catalytic domain. Our data indicate that Fab 3A2 targets the S1' pocket of MMP-14 and directly competes with both substrate and n-TIMP-2 binding (Fig. 4A). Approximately 22% of the Fab 3A2 CDR-H3 residues are positively charged (Lys/Arg/His), suggesting potential interactions between the CDR-H3 loop and the negatively charged active-site vicinity of MMP-14 (Fig. 4B).

The MMP family members are promising drug targets in pathologies ranging from atherosclerosis and stroke to cancer and arthritis. The long CDR-H3 synthetic Fab libraries we constructed have already been applied for the identification of inhibitory antibodies to other MMPs, including MMP-2 and MMP-9. It is highly likely that the general methodology we developed and successfully used in our study could be readily reused to design the selective antibody inhibitors to additional individual MMPs. These selective inhibitors can also be exploited as research tools to shed more light on MMP functionality in normal and pathophysiological conditions. Furthermore, our antibody design technology could be generalized and applied to other targets outside of the MMP family. Overall, our proof-of-principle study suggests that the synthetic antibody

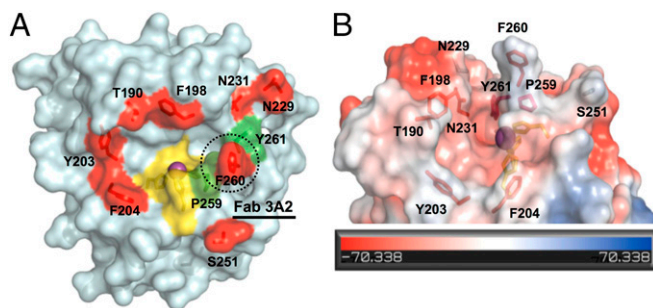


Fig. 4. Inhibition mechanisms by structure interpretation. (A) Top view of the cdMMP-14 reaction site. Three His residues (yellow) of the catalytic motif (HEXXHXXGXXH) coordinate the catalytic zinc (purple). P259, F260, and Y261 (green) form the specific S1' cleft. Eight mutation sites for epitope mapping are shown in red. Competitive ELISA and inhibition assays (Fig. 2F) suggested that Fab 3A2 bound at F260 (black dotted circle). (B) Side view of MMP-14 reaction cleft and vicinity as an electrostatic surface model. Protruding F260 is responsible for the formation of a relatively deep S1' cleft with the catalytic zinc (purple) at the bottom of the cleft. The concave active site is predominantly negatively charged. Images were generated using PyMOL based on the MMP-14 crystal structure (Protein Data Bank 1BQQ).

libraries with the extended CDR-H3 segments have a potential to generate selective function-blocking antibodies to multiple enzymes in which druggable pockets are buried deeply inside the protein globule and which cannot be accessed by the antibodies designed by current methodologies.

Methods

Degenerate polynucleotides encoding the randomized 23-, 25-, and 27-residue-long CDR-H3 segments were chemically synthesized. To mimic the camelid antibody CDR-H3 repertoires, customized XYZ codons were designed (Fig. S2B). The long CDR-H3 fragments were assembled by overlap extension without PCR

amplification (33). Functional full-length CDR-H3 fragments were selected and cloned into phagemids to generate synthetic human Fab libraries. The constructed phage libraries were subjected to three rounds of panning against the immobilized catalytic domain of MMP-14. The isolated Fab clones were biochemically characterized by ELISA, FRET assays, and epitope mapping. Inhibitory function in the cellular context was also tested. Detailed experimental procedures are provided in *SI Methods*.

ACKNOWLEDGMENTS. This work was supported by the National Science Foundation Faculty Early Career Development Program 1453645 (to X.G.), NIH Grant R01 GM115672 (to X.G.), and California Breast Cancer Research Program Developmental and Exploratory Award 211B-0104 (to X.G. and A.Y.S.).

- Overall CM, Kleinfeld O (2006) Tumour microenvironment - opinion: Validating matrix metalloproteinases as drug targets and anti-targets for cancer therapy. *Nat Rev Cancer* 6(3):227–239.
- Liu Y, et al. (2009) Increased matrix metalloproteinase-9 predicts poor wound healing in diabetic foot ulcers. *Diabetes Care* 32(1):117–119.
- Hu J, Van den Steen PE, Sang QX, Opendakker G (2007) Matrix metalloproteinase inhibitors as therapy for inflammatory and vascular diseases. *Nat Rev Drug Discov* 6(6):480–498.
- Elkington PTG, O’Kane CM, Friedland JS (2005) The paradox of matrix metalloproteinases in infectious disease. *Clin Exp Immunol* 142(1):12–20.
- Kawasaki Y, et al. (2008) Distinct roles of matrix metalloproteinases in the early- and late-phase development of neuropathic pain. *Nat Med* 14(3):331–336.
- Dev R, Srivastava PK, Iyer JP, Dastidar SG, Ray A (2010) Therapeutic potential of matrix metalloproteinase inhibitors in neuropathic pain. *Expert Opin Investig Drugs* 19(4):455–468.
- Castro MM, Tanus-Santos JE (2013) Inhibition of matrix metalloproteinases (MMPs) as a potential strategy to ameliorate hypertension-induced cardiovascular alterations. *Curr Drug Targets* 14(3):335–343.
- Deu E, Verdoes M, Bogoy M (2012) New approaches for dissecting protease functions to improve probe development and drug discovery. *Nat Struct Mol Biol* 19(1):9–16.
- Drag M, Salvesen GS (2010) Emerging principles in protease-based drug discovery. *Nat Rev Drug Discov* 9(9):690–701.
- Botkjaer KA, et al. (2016) Development of a specific affinity-matured exosite inhibitor to MT1-MMP that efficiently inhibits tumor cell invasion in vitro and metastasis in vivo. *Oncotarget* 7(13):16773–16792.
- Overall CM, López-Otin C (2002) Strategies for MMP inhibition in cancer: Innovations for the post-trial era. *Nat Rev Cancer* 2(9):657–672.
- Cathcart J, Pulkoski-Gross A, Cao J (2015) Targeting matrix metalloproteinases in cancer: Bringing new life to old ideas. *Genes Dis* 2(1):26–34.
- Turk B (2006) Targeting proteases: Successes, failures and future prospects. *Nat Rev Drug Discov* 5(9):785–799.
- Zucker S, Cao J (2009) Selective matrix metalloproteinase (MMP) inhibitors in cancer therapy: Ready for prime time? *Cancer Biol Ther* 8(24):2371–2373.
- Gialeli C, Theocharis AD, Karamanos NK (2011) Roles of matrix metalloproteinases in cancer progression and their pharmacological targeting. *FEBS J* 278(1):16–27.
- Decock J, Thirkettle S, Wagstaff L, Edwards DR (2011) Matrix metalloproteinases: Protective roles in cancer. *J Cell Mol Med* 15(6):1254–1265.
- Devy L, et al. (2009) Selective inhibition of matrix metalloproteinase-14 blocks tumor growth, invasion, and angiogenesis. *Cancer Res* 69(4):1517–1526.
- Sela-Passwell N, et al. (2011) Antibodies targeting the catalytic zinc complex of activated matrix metalloproteinases show therapeutic potential. *Nat Med* 18(1):143–147.
- Naito S, et al. (2012) Development of a neutralizing antibody specific for the active form of matrix metalloproteinase-13. *Biochemistry* 51(44):8877–8884.
- Sandborn WJ, et al. (2016) Randomised clinical trial: A phase 1, dose-ranging study of the anti-matrix metalloproteinase-9 monoclonal antibody G5-5745 versus placebo for ulcerative colitis. *Aliment Pharmacol Ther* 44(2):157–169.
- Ager EI, et al. (2015) Blockade of MMP14 activity in murine breast carcinomas: implications for macrophages, vessels, and radiotherapy. *J Natl Cancer Inst* 107(4):djv017.
- Fernandez-Catalan C, et al. (1998) Crystal structure of the complex formed by the membrane type 1-matrix metalloproteinase with the tissue inhibitor of metalloproteinases-2, the soluble progelatinase A receptor. *EMBO J* 17(17):5238–5248.
- Lauwereys M, et al. (1998) Potent enzyme inhibitors derived from dromedary heavy-chain antibodies. *EMBO J* 17(13):3512–3520.
- De Genst E, et al. (2006) Molecular basis for the preferential cleft recognition by dromedary heavy-chain antibodies. *Proc Natl Acad Sci USA* 103(12):4586–4591.
- Desmyter A, et al. (1996) Crystal structure of a camel single-domain V-H antibody fragment in complex with lysozyme. *Nat Struct Biol* 3(9):803–811.
- Schmitz KR, Bagchi A, Roovers RC, van Bergen en Henegouwen PM, Ferguson KM (2013) Structural evaluation of EGFR inhibition mechanisms for nanobodies/VHH domains. *Structure* 21(7):1214–1224.
- Hoogenboom HR (2005) Selecting and screening recombinant antibody libraries. *Nat Biotechnol* 23(9):1105–1116.
- Genis L, Gálvez BG, Gonzalo P, Arroyo AG (2006) MT1-MMP: Universal or particular player in angiogenesis? *Cancer Metastasis Rev* 25(1):77–86.
- Morrison CJ, Butler GS, Rodríguez D, Overall CM (2009) Matrix metalloproteinase proteomics: Substrates, targets, and therapy. *Curr Opin Cell Biol* 21(5):645–653.
- Griffin LM, et al. (2014) Analysis of heavy and light chain sequences of conventional camelid antibodies from *Camelus dromedarius* and *Camelus bactrianus* species. *J Immunol Methods* 405:35–46.
- Nguyen VK, Hamers R, Wyns L, Muyldermans S (2000) Camel heavy-chain antibodies: diverse germline V(H)H and specific mechanisms enlarge the antigen-binding repertoire. *EMBO J* 19(5):921–930.
- De Genst E, Saerens D, Muyldermans S, Conrath K (2006) Antibody repertoire development in camelids. *Dev Comp Immunol* 30(1–2):187–198.
- Ge X, Mazor Y, Hunnicke-Smith SP, Ellington AD, Georgiou G (2010) Rapid construction and characterization of synthetic antibody libraries without DNA amplification. *Biotechnol Bioeng* 106(3):347–357.
- Seehaus T, Breiting F, Dübel S, Klewinghaus I, Little M (1992) A vector for the removal of deletion mutants from antibody libraries. *Gene* 114(2):235–237.
- Persson H, et al. (2013) CDR-H3 diversity is not required for antigen recognition by synthetic antibodies. *J Mol Biol* 425(4):803–811.
- Zhang J, et al. (2013) Identification of inhibitory scFv antibodies targeting fibroblast activation protein utilizing phage display functional screens. *FASEB J* 27(2):581–589.
- Farady CJ, Sun J, Darragh MR, Miller SM, Craik CS (2007) The mechanism of inhibition of antibody-based inhibitors of membrane-type serine protease 1 (MT-SP1). *J Mol Biol* 369(4):1041–1051.
- Butler GS, et al. (1999) The specificity of TIMP-2 for matrix metalloproteinases can be modified by single amino acid mutations. *J Biol Chem* 274(29):20391–20396.
- Vandenbroucke RE, Libert C (2014) Is there new hope for therapeutic matrix metalloproteinase inhibition? *Nat Rev Drug Discov* 13(12):904–927.
- Nagase H (2001) Substrate specificity of MMPs. *Matrix Metalloproteinase Inhibitors in Cancer Therapy*, eds Clendeninn NJ, Appelt K (Humana Press, Totowa, NJ), pp 403–420.
- Gupta SP, Patil VM (2012) Specificity of binding with matrix metalloproteinases. *Matrix Metalloproteinase Inhibitors*, ed Gupta SP (Springer, Basel), pp 35–56.
- Nam DH, Ge X (2016) Direct production of functional matrix metalloproteinase-14 without refolding or activation and its application for in vitro inhibition assays. *Biotechnol Bioeng* 113(4):717–723.
- Strongin AY, et al. (1995) Mechanism of cell surface activation of 72-kDa type IV collagenase. Isolation of the activated form of the membrane metalloproteinase. *J Biol Chem* 270(10):5331–5338.
- Golubkov VS, et al. (2006) Membrane type-1 matrix metalloproteinase confers aneuploidy and tumorigenicity on mammary epithelial cells. *Cancer Res* 66(21):10460–10465.
- Liu T, et al. (2015) Rational design of antibody protease inhibitors. *J Am Chem Soc* 137(12):4042–4045.
- Zhang Y, et al. (2013) Functional antibody CDR3 fusion proteins with enhanced pharmacological properties. *Angew Chem Int Ed Engl* 52(32):8295–8298.
- Schneider EL, et al. (2012) A reverse binding motif that contributes to specific protease inhibition by antibodies. *J Mol Biol* 415(4):699–715.
- Wu Y, et al. (2007) Structural insight into distinct mechanisms of protease inhibition by antibodies. *Proc Natl Acad Sci USA* 104(50):19784–19789.
- Ganesan R, et al. (2009) Unraveling the allosteric mechanism of serine protease inhibition by an antibody. *Structure* 17(12):1614–1624.
- Wu TT, Johnson G, Kabat EA (1993) Length distribution of CDRH3 in antibodies. *Proteins* 16(1):1–7.
- Shiryayev SA, et al. (2013) A monoclonal antibody interferes with TIMP-2 binding and incapacitates the MMP-2-activating function of multifunctional, pro-tumorigenic MMP-14/MT1-MMP. *Oncogenesis* 2:e80.
- Nam DH, Ge X (2013) Development of a periplasmic FRET screening method for protease inhibitory antibodies. *Biotechnol Bioeng* 110(11):2856–2864.
- Pardon E, et al. (2014) A general protocol for the generation of nanobodies for structural biology. *Nat Protoc* 9(3):674–693.
- Fellouse FA, Sidhu SS (2013) Making antibodies in bacteria. *Making and Using Antibodies*, ed Kase MR (CRC Press, Boca Raton, FL), pp 151–172.
- Knight CG, Willenbrock F, Murphy G (1992) A novel coumarin-labelled peptide for sensitive continuous assays of the matrix metalloproteinases. *FEBS Lett* 296(3):263–266.
- Dunbar J, et al. (2016) SabPred: A structure-based antibody prediction server. *Nucleic Acids Res* 44(W1):W474–W478.